Biochemical and Biophysical Research Communications 452 (2014) 588–592

Contents lists available at ScienceDirect

Biochemical and Biophysical Research Communications

journal homepage: www.elsevier.com/locate/ybbrc

Low-mass molecular dynamics simulation: A simple and generic technique to enhance configurational sampling

Yuan-Ping Pang *

Computer-Aided Molecular Design Laboratory, Mayo Clinic, Rochester, MN 55905, USA

ARTICLE INFO

Article history:
Received 14 August 2014
Available online 30 August 2014

Keywords:
Configurational sampling enhancement
Isothermal–isobaric ensemble
Protein folding
Fast-folding miniature protein
Chignolin analogue
β-Hairpin

ABSTRACT

CLN025 is one of the smallest fast-folding proteins. Until now it has not been reported that CLN025 can autonomously fold to its native conformation in a classical, all-atom, and isothermal–isobaric molecular dynamics (MD) simulation. This article reports the autonomous and repeated folding of CLN025 from a fully extended backbone conformation to its native conformation in explicit solvent in multiple 500-ns MD simulations at 277 K and 1 atm with the first folding event occurring as early as 66.1 ns. These simulations were accomplished by using AMBER forcefield derivatives with atomic masses reduced by 10-fold on Apple Mac Pros. By contrast, no folding event was observed when the simulations were repeated using the original AMBER forcefields of FF12SB and FF14SB. The results demonstrate that low-mass MD simulation is a simple and generic technique to enhance configurational sampling. This technique may propel autonomous folding of a wide range of miniature proteins in classical, all-atom, and isothermal–isobaric MD simulations performed on commodity computers—an important step forward in quantitative biology.

1. Introduction

CLN025 is one of the smallest fast-folding proteins that folds into a β-hairpin with a sequence of YYDPETGTWY according to both its X-ray crystal and nuclear magnetic resonance (NMR) structures (Fig. 1A and B) [1]. Autonomous and repeated folding of CLN025 has been observed in a classical, all-atom, canonical, and 106-μs molecular dynamics (MD) simulation performed on a one-of-a-kind, proprietary, special-purpose computer [2]. This article reports the use of low atomic masses to speed up configurational sampling in MD simulations and its successful application to autonomous folding of CLN025 in classical, all-atom, isothermal–isobaric, and 500-ns MD simulations with TIP3P water [3] at the same temperature and pressure conditions (277 K and 1 atm) as those used for the experimental folding study of CLN025 [1].

2. Materials and methods

2.1. Folding simulation protocol

A fully extended backbone conformation of CLN025 was generated by MacPyMOL Version 1.5.0 (Schrödinger LLC, Portland, OR) and solvated with 1532 TIP3P water molecules to keep the closest distance between any atom of CLN025 and the edge of the periodic solvent box at 8.2 Å using LEAP of AmberTools 1.5 (University of California, San Francisco). Because pH 5.7 was used for the NMR structure determination for CLN025 [1], two sodium ions were added for neutrality of the protein. Four sodium chloride molecules were also added to keep the ionic strength of the system at ~143 mM NaCl. Although the ionic strength used for the NMR study was 20 mM Na_3PO_4 [1], in this study ~143 mM NaCl was used to minimize the intermolecular interaction of CLN025 with its periodic image during the MD simulations. Using FF12SB or its derivatives as described in Section 3, the solvated and slightly brined CLN025 was then energy-minimized for 100 cycles of steepest-descent minimization followed by 900 cycles of conjugate-gradient minimization to remove close van der Waals contacts using SANDER of AMBER 11 (University of California, San Francisco), heated from 0 to 277 K at a rate of 10 K/ps under constant temperature and volume, and finally simulated in ten independent MD

Abbreviations: MD, molecular dynamics; LMD, low-mass molecular dynamics; NMR, nuclear magnetic resonance; CαβRMSD, Cα and Cβ root mean square deviation; CRMSD, all carbon atom root mean square deviation.

* Address: Stabile 12-26, Mayo Clinic, 200 First Street SW, Rochester, MN 55905, USA.

E-mail address: pang@mayo.edu

http://dx.doi.org/10.1016/j.bbrc.2014.08.119
0006-291X/

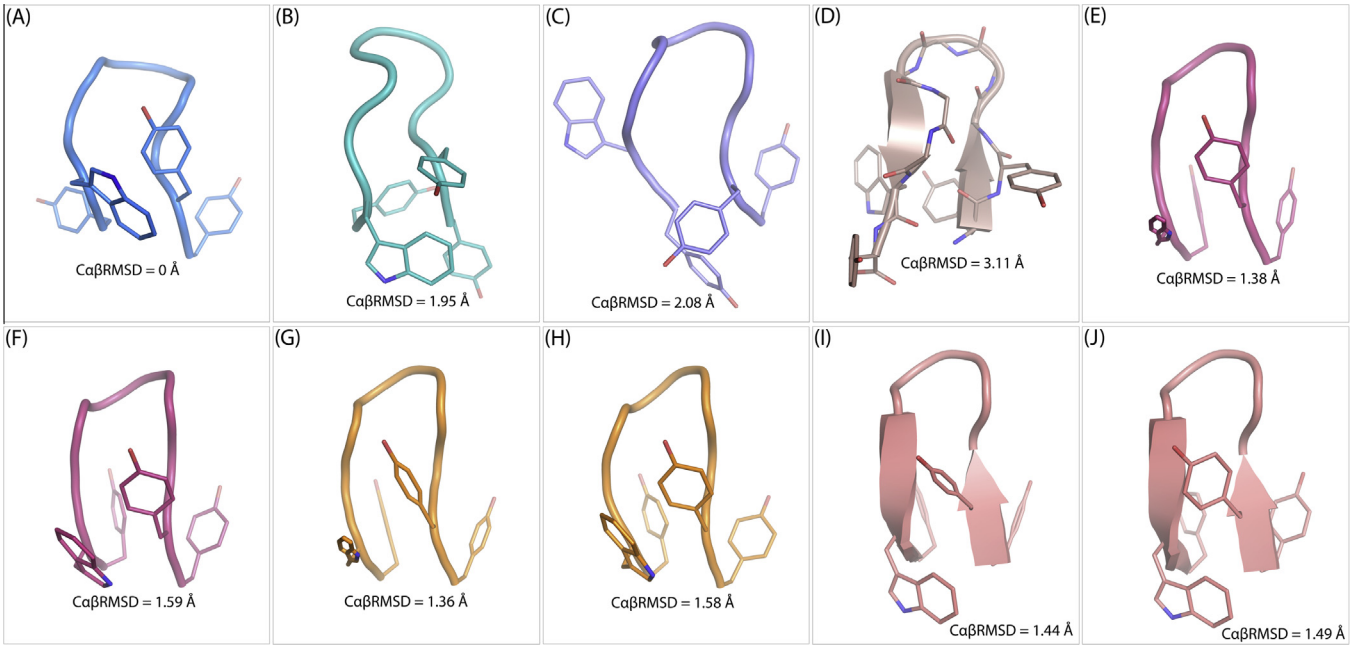

Fig. 1. Native and native-like conformations of CLN025 obtained from experimental and computational studies and their Cα and Cβ root mean square deviations (CαβRMSDs). (A) The NMR structure [1]. (B) The crystal structure [1]. (C) A native-like conformation obtained from simulations using FF12SBlm. (D) Another native-like conformation obtained from simulations using FF12SBlm. (E) The time-averaged conformation of the largest cluster of conformations obtained from the simulations using FF12SBlm. (F) The representative conformation of the largest cluster of conformations obtained from simulations using FF12SBlm. (G) The time-averaged conformation of the largest cluster of conformations obtained from the simulations using FF14SBlm. (H) The representative conformation of the largest cluster of conformations obtained from the simulations using FF14SBlm. (I): The time-averaged conformation of the second largest cluster of conformations obtained from the simulations using FF14SBlm. (J) The representative conformation of the second largest cluster of conformations obtained from the simulations using FF14SBlm.

simulations using PMEMD of AMBER 11 with a periodic boundary condition at a constant temperature of 277 K and a constant pressure of 1 atm with isotropic molecule-based scaling. The ten unique seed numbers for initial velocities of Simulations 1–10 are 1804289383, 846930886, 1681692777, 1714636915, 1957747793, 424238335, 719885386, 1649760492, 596516649, and 1189641421, respectively. All simulations used (1) a dielectric constant of 1.0, (2) the Berendsen coupling algorithm [4], (3) the Particle Mesh Ewald method to calculate long-range electrostatic interactions [5], (4) a time step of 1.0 fs, (5) SHAKE-bond-length constraints applied to all the bonds involving the H atom, (6) a protocol to save the image closest to the middle of the "primary box" to the restart and trajectory files, (7) a formatted restart file, and (8) default values of all other inputs of PMEMD. Each simulation was performed on a 12-core Apple Mac Pro with Intel Westmere (2.40/2.93 GHz). Trajectories were saved at 100-ps intervals in all simulations.

2.2. Folding simulation analysis

The native conformations of CLN025 in the NMR and crystal structures have Tyr2 and Trp9 on one side of the β-sheet and Tyr1 and Tyr10 on the other side [1] (Fig. 1A and B). Interestingly, analysis of the trajectories obtained from MD simulations showed that CLN025 could fold to native-like β-hairpins with Tyr1, Trp9, and Tyr10 on one side of the β-sheet and Tyr2 on the other side (Fig. 1C) or with Tyr1 and Trp9 on one side and Tyr2 and Tyr10 on the other side (Fig. 1D). The lowest Cα and Cβ root mean square deviation (CαβRMSD) between one of the native-like β-hairpins and the NMR structure is 2.08 Å, whereas the corresponding Cα root mean square deviation is 1.33 Å. The CαβRMSD between the NMR and crystal structures is 1.95 Å. Therefore, to distinguish the native β-hairpins from the native-like ones, conformations with CαβRMSDs of $\leqslant$1.96 Å relative to the NMR structure are considered to be at the native or folded state.

A folding event of CLN025 in an MD simulation is delineated by (1) a smoothed curve of CαβRMSD over simulation time (Fig. 2), (2) an average folding time (Table 1), and (3) an overall native-state population (Table 1). The smoothed curves were generated by the PRISM program from GraphPad Software (La Jolla, California) using 32 neighbors on each size and 6th order of the smoothing polynomial. The native-state population of a simulation is the number of conformations with CαβRMSDs of $\leqslant$1.96 Å divided by all conformations obtained from the simulation. If the native-state population of a simulation is $\leqslant$1.5%, the conformations with CαβRMSDs of $\leqslant$1.96 Å are considered to be too transient to constitute a folding event. In other words, if a simulation captures a folding event, the native-state population of this simulation must be >1.5%. The overall native-state population is the number of conformations with CαβRMSDs of $\leqslant$1.96 Å obtained from a set of simulations divided by all conformations of the set. A folding time—defined as the time to fold a protein from a fully extended backbone conformation to its native conformation—is obtained from the first time when CαβRMSD reaches $\leqslant$1.96 Å in a simulation that must have its native-state population of >1.5%. If a simulation does not capture a folding event, the folding time is considered to be greater than the entire simulation time.

The average folding time and the overall native-state population of a set of simulations are provided to complement the smoothed CαβRMSD-vs-time curve that does not display short folding events. Although the smoothed CαβRMSD-vs-time curve is informative with regard to unfolding and refolding events in a simulation, its limitation is that display of CαβRMSD-vs-time curves for a set of simulations requires too much page space. By definition, the overall native-state population is less stochastic than the average folding time. Therefore, the overall native-state population is a better descriptor of protein folding in multiple MD simulations than the CαβRMSD-vs-time curve or the average folding time.

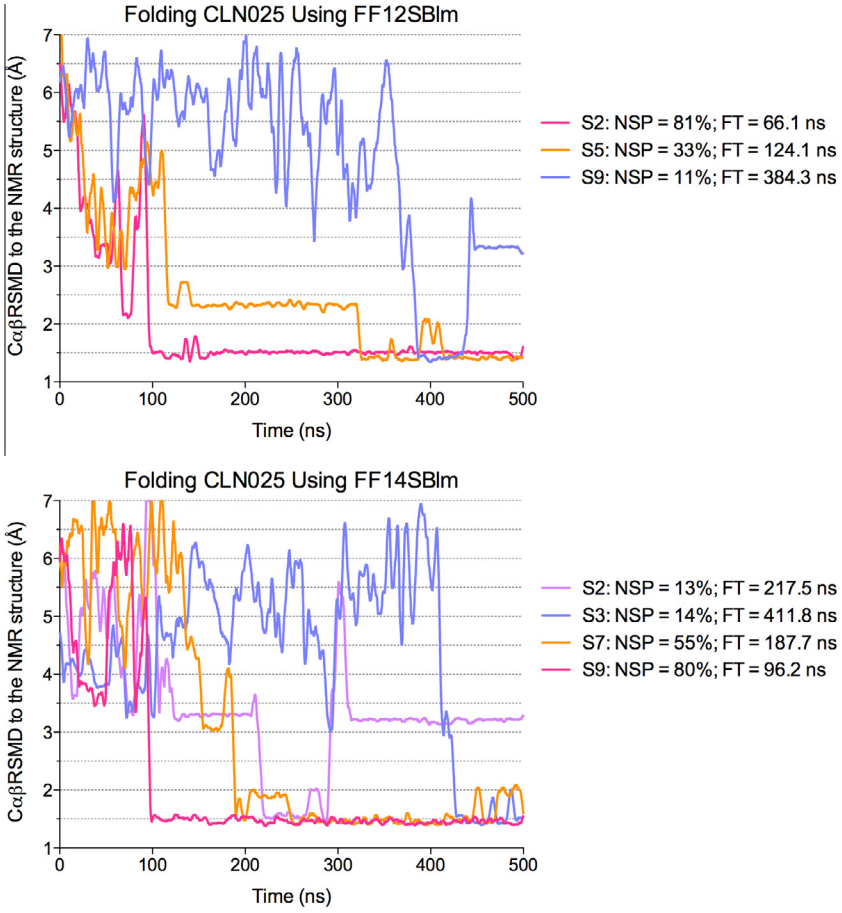

Fig. 2. Smoothed time series of Cα and Cβ root mean square deviation (CαβRMSD) of CLN025. *SN*: Simulation *N*. NSP: Native-state population. FT: Folding time.

Table 1
Folding of CLN025 in 500-ns molecular dynamics simulations with TIP3P Water at 277 K and 1 atm.

Forcefield	Number of simulations	Number of simulations with a folding event	Overall native-state population (%)	Average folding time (ns)
FF12SB	10	0	0	>500
FF14SB	10	0	0	>500
FF12SBlm	10	3	13	>407.4
FF14SBlm	10	4	16	>391.3

2.3. Cluster analysis and coordinate deviation calculations

A two-step cluster analysis of the CLN025 trajectories obtained from MD simulations that captured a folding event was performed using PTRAJ of AmberTools 1.5 with the average-linkage algorithm [6]. Cluster analysis of 13,200 trajectories saved at 100-ps intervals during the 61–500 ns period of Simulations 2, 5, and 9 using FF12SBlm was first done using epsilon of 2.0 Å and root mean square coordinate deviation on Cα of residues 1–10. All the trajectories in the most populated cluster were then clustered using epsilon of 2.0 Å and root mean square coordinate deviation on all carbon atoms of residues 1, 2, 9, and 10. A total of 16,164 trajectories saved at 100-ps intervals during the 96–500 ns period of Simulations 2, 3, 7, and 9 using FF14SBlm were clustered using the same protocol as the one for the FF12SBlm trajectories. CαβRMSDs, Cα root mean square deviations, and all carbon atom root mean square deviations (CRMSDs) were calculated automatically using PTRAJ of AmberTools 1.5 or manually using ProFit V2.6 (http://www.bioinf.org.uk/software/profit/).

3. Results and discussion

3.1. Low-mass molecular dynamics simulation

An MD simulation is designed to computationally simulate the time-dependent behavior of a system of particles by solving Newton's equations of motion for all the particles as a function of time [7]. In an MD simulation, the product of the particle mass and the particle acceleration is calculated as the derivative of the potential energy of the particle with respect to its position ($m_i a_i = -\delta E_i/\delta r_i$). When all particle masses of the system are purposefully reduced, accelerations of all the particles increase, and consequently the transition time from one configuration to the other decreases. This reasoning inspired the use of low atomic masses to speed up configurational sampling in MD simulations.

Bonds, except for those involving hydrogen, cannot be constrained in MD simulations when using MD simulation programs with high parallel-computing efficiency such as PMEMD. Because of this limitation, masses of heavy atoms cannot be set too low, otherwise a time step of <1.0 fs has to be used to avoid system instability. The speed of an MD simulation is inversely related to the time step used in the simulation. There is an intricate balance between the desire to decrease atomic masses and the desire to increase time step. After years of performing low-mass MD (LMD) simulations with various proteins including metalloproteins [8–19], this author finds that reducing atomic masses by 10-fold

offers substantial enhancement of configurational sampling in MD simulations with a time step of 1.0 fs and a temperature of ⩽340 K without compromising system stability.

The substantial enhancement of configurational sampling of LMD simulation is demonstrated below by the inability to autonomously fold CLN025 in MD simulations using current AMBER forcefields FF12SB [20] and FF14SB [21] and the ability to autonomously fold CLN025 in MD simulations using FF12SBlm and FF14SBlm that are revised from FF12SB and FF14SB, respectively, by reducing atomic masses by an order of magnitude.

3.2. Autonomous folding of CLN025 by FF12SBlm or FF14SBlm

As shown in Fig. 2 and Table 1, FF12SBlm was able to fold CLN025 from a fully extended backbone conformation to its NMR structure in three out of ten classical, all-atom, isothermal–isobaric, and 500-ns MD simulations at 277 K and 1 atm with an overall native-state population of 13% and an average folding time of >407.4 ns (Table 1). The shortest folding time of the three simulations shown in Fig. 2 is 66.1 ns.

To confirm the folding events and to obtain time-averaged structures for insight into side-chain mobility of CLN025 in the folded state, a cluster analysis of all the trajectories of CLN025 saved at 100-ps intervals during the 61–500 ns period of Simulations 2, 5, and 9 was performed using root mean square coordinate deviation of Cα between two CNL025 trajectories. According to this analysis, there are a total of 149 clusters. Of these clusters, only one cluster is highly populated and has 9142 conformations that account for 69.3% of all 13,200 conformations used in the cluster analysis. All other clusters have populations of ⩽1.7%. Using mean square coordinate deviation of all carbon atoms of residues 1, 2, 9, and 10 between two CNL025 trajectories, a cluster analysis of all conformations of the most populated cluster identified ten sub-clusters with populations of >1.0%. The most populated sub-cluster has 5140 conformations accounting for 56.2% of all conformation in the most populated cluster. All other sub-clusters have populations of ⩽10.0%.

The time-averaged conformation of the most populated sub-cluster has a CαβRMSD of 1.38 Å relative to the NMR structure. As shown in Fig. 1E, the side chains of Tyr1, Trp9, and Try10 are highly contracted in the time-averaged conformation, suggesting that the side chains of residues 1, 9, and 10 are more mobile than that of residue 2 at the folded state. The representative conformation of this sub-cluster has a CαβRMSD of 1.59 Å relative to the NMR structure (Fig. 1F). The time-averaged and representative conformations have CRMSDs of 1.80 Å and 2.11 Å relative to the NMR structure, respectively. Interestingly, when compared to the crystal structure of CLN025 [1], the corresponding CRMSDs increase to 2.80 Å and 2.90 Å, respectively. These results show that FF12SBlm is able to autonomously fold CLN025 in water to conformations that resemble more the solution NMR structure than the solid crystal structure.

Using 2000 conformations saved at 100-ps intervals during the 200-ns period of Simulation 2, a video was made to unequivocally demonstrate the ability of FF12SBlm to autonomously fold CLN025 in a classical, all-atom, isothermal–isobaric, and 500-ns MD simulation with TIP3P water [3] at 277 K and 1 atm (Video S1). Consistent with the observed contractions of three aromatic side chains of the time-averaged conformation shown in Fig. 1E, Video S1 shows spinning of the two terminal phenolic rings and rotation of the indole ring.

Under the same simulation conditions, FF14SBlm folded CLN025 in four out of ten MD simulations with an overall native-state population of 16% and an average folding time of >391.3 ns (Fig. 2, Table 1, and Video S2). The shortest folding time of the four simulations shown in Fig. 2 is 96.2 ns. Following the procedure described above, the first-step clustering identified 181 clusters. One cluster has 11,486 conformations (71.1%). All other clusters have populations of ⩽2.1%. The second-step clustering identified three sub-clusters with populations of >8.5%. Sub-clusters 25, 7, and 1 have 3879 (33.8%), 2490 (21.7%), and 2446 (21.3%) conformations, respectively. The conformations in the two most-populated sub-clusters represent the native β-hairpins, while the conformations in the least populated sub-cluster represent one of the native-like β-hairpins. Relative to the NMR structure, the time-averaged and representative conformations of Sub-clusters 25, 7, and 1 have CRMSDs of 1.76 Å and 2.16 Å, 1.78 Å and 1.95 Å, and 4.95 Å and 4.96 Å, respectively. Relative to the crystal structure, the corresponding CRMSDs change to 2.76 Å and 2.96 Å, 2.09 Å and 2.27 Å, and 4.52 Å and 4.67 Å, respectively. These results show that FF14SBlm is also able to autonomously fold CLN025 in water to conformations that resemble more the solution NMR structure than the solid crystal structure.

Interestingly, the time-averaged conformation of the most populated sub-cluster (Fig. 1G) shows substantial contractions of all four aromatic side chains of CLN025. These contractions are different from the contractions observed in the simulations using FF12SBlm and suggest that the side chains of residues 1, 9, and 10 are as mobile as that of residue 2 at the folded state. The difference with regard to the mobility of Tyr2 between the simulations using FF12SBlm and FF14SBlm reveals the sensitivity of sub-microsecond LMD simulations to side-chain torsion forcefield parameters.

3.3. Configurational sampling enhancement

Under the same simulation conditions, none of the simulations using FF12SB or FF14SB captured a folding event. By contrast, FF12SBlm and FF14SBlm folded CLN025 in three and four out of ten 500-ns MD simulations at 277 K and 1 atm with overall native-state populations of 13% and 16%, respectively. The average folding times observed in the simulations using FF12SBlm and FF14SBlm are >407.4 ns and >391.3 ns, respectively. These results demonstrate substantial enhancement of configurational sampling in LMD simulations. In addition, the results of the LMD simulations indicate that CLN025 will likely fold in an MD simulation using FF12SB or FF14SB, if the duration of the simulation is extended by 10-fold. The results also show that FF14SB is an improved forcefield for autonomous folding of CLN025 over FF12SB.

3.4. Advantages and disadvantages of LMD simulation

Because LMD simulation uses 0.1008 Da for hydrogen, there are disadvantages with this technique. All bonds involving hydrogen must be constrained in an LMD simulation. To avoid system instability caused by long time steps or by high temperatures, the time step and temperature used in an LMD simulation must be ⩽1.0 fs and ⩽340 K. The kinetics obtained from LMD simulations cannot be compared directly to the kinetics determined experimentally, although the relative kinetics of two systems can be compared to the corresponding experimental data. To perform an LMD simulation on a graphics-processing unit, there is the inconvenience of recompiling PMEMD_CUDA of AMBER 12 (University of California, San Francisco) using 0.1008 Da for hydrogen. Preliminary studies using PMEMD_CUDA of AMBER 12 suggest that the system be equilibrated first on a central processing unit and then simulated on a graphics-processing unit.

Nevertheless, temperatures of biological systems rarely exceed 340 K, and in theory the improvement of configurational sampling in LMD simulations is approximately 10 fold. To perform LMD simulations using the AMBER package [21], all that is required is an frcmod file with atomic masses reduced by 10-fold. The LMD simulation technique is not restricted to the AMBER forcefield, and it

can be used in conjunction with other sampling enhancement techniques to achieve even a higher efficiency of configurational sampling. For example, when LMD simulation is combined with techniques that lower potential energy barriers by shortening C—H bonds and zeroing protein backbone torsion potentials to accelerate sampling, autonomous folding of a tryptophan zipper [22], a tryptophan cage [23], a villin headpiece subdomain [24], and a zinc finger analog [25] can be simulated in classical, all-atom, isothermal–isobaric, and 300-ns MD simulations performed on Apple Mac Pros (Y.-P. Pang's unpublished work). In addition, the LMD simulation technique is not restricted to protein folding; it can be applied to homology protein structure refinement, simulations of ligand–receptor complexation and allosteric modulation, drug free energy binding calculations, and simulations of polynucleotides and non-biological substances. As a simple and generic configurational sampling enhancement technique, LMD simulations may propel autonomous folding of a wide range of miniature proteins in classical, all-atom, and isothermal–isobaric MD simulations performed on commodity computers—an important step forward in quantitative biology.

Disclaimer

The contents of this article are the sole responsibility of the author and do not necessarily represent the official views of the funders.

Acknowledgments

The author acknowledges the support of this work from the US Defense Advanced Research Projects Agency (DAAD19-01-1-0322), the US Army Medical Research Material Command (W81XWH-04-2-0001), the US Army Research Office (DAAD19-03-1-0318 and W911NF-09-1-0095), the US Department of Defense High Performance Computing Modernization Office, and the Mayo Foundation for Medical Education and Research. The author also greatly appreciates the comments from an anonymous reviewer.

Appendix A. Supplementary data

Supplementary data associated with this article can be found, in the online version, at http://dx.doi.org/10.1016/j.bbrc.2014.08.119.

References

[1] S. Honda, T. Akiba, Y.S. Kato, Y. Sawada, M. Sekijima, M. Ishimura, A. Ooishi, H. Watanabe, T. Odahara, K. Harata, Crystal structure of a ten-amino acid protein, J. Am. Chem. Soc. 130 (2008) 15327–15331.
[2] K. Lindorff-Larsen, S. Piana, R.O. Dror, D.E. Shaw, How fast-folding proteins fold, Science 334 (2011) 517–520.
[3] W.L. Jorgensen, J. Chandreskhar, J.D. Madura, R.W. Impey, M.L. Klein, Comparison of simple potential functions for simulating liquid water, J. Chem. Phys. 79 (1983) 926–935.
[4] H.J.C. Berendsen, J.P.M. Postma, W.F. van Gunsteren, A. Di Nola, J.R. Haak, Molecular dynamics with coupling to an external bath, J. Chem. Phys. 81 (1984) 3684–3690.
[5] T.A. Darden, D.M. York, L.G. Pedersen, Particle mesh Ewald: An N log(N) method for Ewald sums in large systems, J. Chem. Phys. 98 (1993) 10089–10092.
[6] J. Shao, S.W. Tanner, N. Thompson, T.E. Cheatham III, Clustering molecular dynamics trajectories: 1. Characterizing the performance of different clustering algorithms, J. Chem. Theory Comput. 3 (2007) 2312–2334.
[7] M.P. Allen, D.J. Tildesley, Computer Simulation of Liquids, Oxford University Press, New York, US, 1994.
[8] Y.-P. Pang, Novel zinc protein molecular dynamics simulations: Steps toward antiangiogenesis for cancer treatment, J. Mol. Model. 5 (1999) 196–202.
[9] Y.-P. Pang, K. Xu, J. El Yazal, F.G. Prendergast, Successful molecular dynamics simulation of the zinc-bound farnesyltransferase using the cationic dummy atom approach, Protein Sci. 9 (2000) 1857–1865.
[10] Y.-P. Pang, Successful molecular dynamics simulation of two zinc complexes bridged by a hydroxide in phosphotriesterase using the cationic dummy atom method, Proteins 45 (2001) 183–189.
[11] H. Sun, J. El Yazal, O. Lockridge, L.M. Schopfer, S. Brimijoin, Y.-P. Pang, Predicted Michaelis–Menten complexes of cocaine-butyrylcholinesterase – Engineering effective butyrylcholinesterase mutants for cocaine detoxication, J. Biol. Chem. 276 (2001) 9330–9336.
[12] Y.-P. Pang, Three-dimensional model of a substrate-bound SARS chymotrypsin-like cysteine proteinase predicted by multiple molecular dynamics simulations: Catalytic efficiency regulated by substrate binding, Proteins 57 (2004) 747–757.
[13] J.G. Park, P.C. Sill, E.F. Makiyi, A.T. Garcia-Sosa, C.B. Millard, J.J. Schmidt, Y.-P. Pang, Serotype-selective, small-molecule inhibitors of the zinc endopeptidase of botulinum neurotoxin serotype A, Bioorg. Med. Chem. 14 (2006) 395–408.
[14] Y.-P. Pang, Novel acetylcholinesterase target site for malaria mosquito control, PLoS ONE 1 (2006) e58.
[15] Y.-P. Pang, Species marker for developing novel and safe pesticides, Bioorg. Med. Chem. Lett. 17 (2007) 197–199.
[16] B.J. Killian, J.Y. Kravitz, S. Somani, P. Dasgupta, Y.-P. Pang, M.K. Gilson, Configurational entropy in protein-peptide binding: Computational study of Tsg101 ubiquitin E2 variant domain with an HIV-derived PTAP nonapeptide, J. Mol. Biol. 389 (2009) 315–335.
[17] F. Ekström, A. Hörnberg, E. Artursson, L.-G. Hammarström, G. Schneider, Y.-P. Pang, Structure of HI-6•sarin-acetylcholinesterase determined by X-ray crystallography and molecular dynamics simulation: Reactivator mechanism and design, PLoS ONE 4 (2009) e5957.
[18] T. Althoff, D.J. Mills, J.L. Popot, W. Kuhlbrandt, Arrangement of electron transport chain components in bovine mitochondrial supercomplex I1III2IV1, EMBO J. 30 (2011) 4652–4664.
[19] Y.-P. Pang, H. Dai, A. Smith, X.W. Meng, P.A. Schneider, S.H. Kaufmann, Bak conformational changes induced by ligand binding: Insight into BH3 domain binding and Bak homo-oligomerization, Sci. Rep. 2 (2012) 257.
[20] D.A. Case, T.A. Darden, T.E. Cheatham III, C.L. Simmerling, J. Wang, R.E. Duke, R. Luo, R.C. Walker, W. Zhang, K.M. Merz, Jr., B. Roberts, S. Hayik, A. Roitberg, G. Seabra, J. Swails, A.W. Goetz, I. Kolossvary, K.F. Wong, F. Paesani, J. Vanicek, R.M. Wolf, J. Liu, X. Wu, S.R. Brozell, T. Steinbrecher, H. Gohlke, Q. Cai, X. Ye, J. Wang, M.-J. Hsieh, G. Cui, D.R. Roe, D.H. Mathews, M.G. Seetin, R. Salomon-Ferrer, C. Sagui, V. Babin, T. Luchko, S. Gusarov, A. Kovalenko, P.A. Kollman, The FF12SB force field, AmberTools 13 Reference Manual (2013) 27–29.
[21] D.A. Case, V. Babin, J.T. Berryman, R.M. Betz, Q. Cai, D.S. Cerutti, T.E. Cheatham III, T.A. Darden, R.E. Duke, H. Gohlke, A.W. Goetz, S. Gusarov, N. Homeyer, P. Janowski, J. Kaus, I. Kolossvary, A. Kovalenko, T.S. Lee, S. LeGrand, T. Luchko, R. Luo, B. Madej, K.M. Merz, Jr., F. Paesani, D.R. Roe, A. Roitberg, C. Sagui, R. Salomon-Ferrer, G. Seabra, C.L. Simmerling, W.L. Smith, J. Swails, R.C. Walker, J. Wang, R.M. Wolf, X. Wu, P.A. Kollman, The FF14SB force field, AMBER 14 Reference Manual (2014) 29–31.
[22] A.G. Cochran, N.J. Skelton, M.A. Starovasnik, Tryptophan zippers: Stable, monomeric beta-hairpins, Proc. Natl. Acad. Sci. USA 98 (2001) 5578–5583.
[23] B. Barua, J.C. Lin, V.D. Williams, P. Kummler, J.W. Neidigh, N.H. Andersen, The Trp-cage: Optimizing the stability of a globular miniprotein, Protein Eng. Des. Sel. 21 (2008) 171–185.
[24] C.J. McKnight, P.T. Matsudaira, P.S. Kim, NMR structure of the 35-residue villin headpiece subdomain, Nat. Struct. Biol. 4 (1997) 180–184.
[25] C.A. Sarisky, S.L. Mayo, The ββα fold: Explorations in sequence space, J. Mol. Biol. 307 (2001) 1411–1418.